Applied Surface Science 254 (2008) 7431–7437

Contents lists available at ScienceDirect

Applied Surface Science

journal homepage: www.elsevier.com/locate/apsusc

# Statistical analysis of paper surface microstructure: A multi-scale approach

Pierre Vernhes *, Jean-Francis Bloch, Christophe Mercier, Anne Blayo, Bernard Pineaux

*EFPG, 461 rue de la papeterie, BP 65, 38402 Saint-Martin d'Hères, France*

ARTICLE INFO

*Article history:*
Received 8 February 2008
Received in revised form 30 May 2008
Accepted 1 June 2008
Available online 17 June 2008

*Keywords:*
Surface topography
Multi-scale analysis
Fractal analysis
Focus variation technique

ABSTRACT

Paper properties such as gloss, friction or printability strongly depend on the surface roughness. However, this dependence on the roughness in relation to the measurement scale is not systematically taken into account. Paper surface topography is here studied in a multi-scale approach with the help of a focus variation device. For each measurement scale, statistical parameters were calculated to describe the surface. We isolated among the long list of parameters calculated those that were relevant for paper surface topography analysis. A new method of characterization of paper surface roughness is proposed based on a scaling analysis taken from either profile or surface data. Depending on the scale of analysis different fractal stages were exhibited. The influence of the step of discretization on the roughness parameters was also investigated.



## 1. Introduction

Paper is a complex composite material. Its structure and its surface greatly influence its runnability and its printability [1]. The roughness is primordial for the absorption and the spreading of inks [2] or to determine the amount of coating. The paper surface characterization is crucial for understanding light reflection and scattering that control the level of gloss [3–10]. The paper surface topography can be described with different techniques, such as air leakage instruments, stylus technique or optical devices [11–14] including scanning electron microscopy (SEM), atomic force microscopy (AFM), confocal laser scanning microscopy (CLSM), laser profilometer, interferometry and chromatic aberration. An optical device based on the focus variation technique allows for the mapping of the paper surface with a sub-micron precision [15]. From this mapping, statistical parameters can be calculated according to TAPPI (or ISO) standard. A huge number of parameters exists; the most common is the root mean square of the height distribution of the surface, $S_q$. Nevertheless, it appears insufficient to approach the complexity of the paper surface topography. The material volume and void volume in the surface bearing area are complementary geometrical descriptors of a surface topography [16]. The material volume and void volume enclosed in the contacting surface of the material may have a close relation with functional properties of the surface, such as bearing, wear and fluid retention. Special attention was therefore accorded to these parameters.

Different types of data processing such as filters were used to characterize the paper surface quality. Hence, fast Fourier transform (FFT) can be performed to separate the small-scale variation from the large scale. Gaussian filtering in the spatial domain allows for the decomposition of the structure into different wavelength ranges [10]. Recently the fractal dimension was also used to identify the paper irregularities [17].

The distributions of the facet orientation have also been related to the gloss level [9]. Hence the multiple surface scattering was related to the local slope of each facet and its orientation [18]. This method also allows discriminating smooth part of the surface, that is to say local glossy region. Paper is a multi-scale material [19,20]. Like other materials, the value of paper roughness is strongly dependent on the evaluation length [21] and on the discretization step [22,23]. However the influence of these two factors was systematically taken into account to characterize paper surface.

The aim of this paper is to study the paper surface topography in a multi-scale approach. Thanks to a focus variation device (IFM from Alicona®), we studied the paper surface properties of five paper samples at different magnifications (×5, ×10, ×20, ×50 and ×100). Thus, paper topography was characterized with surface sizes varying from 80 μm × 80 μm with a spacing of 40 nm to a size of 1.6 mm × 1.6 mm with a spacing of 1.6 μm. The technology on which the system is based has recently been included into ISO standards [24] classifying different methods for surface texture extraction. For each magnification, statistical study of the standard parameters was performed according to the paper quality. Hence,

* Corresponding author.
*E-mail addresses:* Pierre.vernhes@efpg.inpg.fr (P. Vernhes), Jean-francis.bloch@efpg.inpg.fr (J.-F. Bloch), christophemercier@club-internet.fr (C. Mercier), Anne.blayo@efpg.inpg.fr (A. Blayo), Bernard.pineaux@efpg.inpg.fr (B. Pineaux).

0169-4332/$ – see front matter © 2008 Elsevier B.V. All rights reserved.
doi:10.1016/j.apsusc.2008.06.023

it was possible to isolate among the large list of parameters those who effectively enable a discrimination of paper grades, while being reproducible.

In a second part, statistical methods were investigated to depict the dependency of the roughness parameters to both, the length of analysis and to the step of discretization. Therefore, a new statistical approach is suggested to describe the evolution of paper surface roughness in relation to the scaling length at a given discretization step. Different fractal stages are exhibited.

## 2. Materials and methods

### 2.1. Physical paper properties of the samples

We chose two offices papers referenced as Q+ and Q−, respectively. These papers are common office papers: Q+ is assumed to have a better quality than Q−. We also studied two inkjet papers, one of high quality (used for photographic purpose) referenced as JET+ and a more common, referenced as JET−. Finally a coated paper was also analysed (referenced as C).

Paper properties (basis weight, thickness and Bekk roughness, PPS and Bendtsen) were measured (Table 1).

### 2.2. Description of the infinite focus measurement machine

The infinite focus measurement (IFM) machine is an optical measurement device. It allows for the acquisition of dataset at high depth of focus similar to the SEM.

The main component of this optical metrology instrument is a precision optic consisting of various lens systems. It can be equipped with different objectives allowing measurements with different resolutions. With a beam splitting mirror, light emerging from a white light source is inserted into the optical path of the system and focused onto the specimen via the objective. Depending on the topography of the specimen, the light is reflected into several directions as soon as it hits the specimen. All rays emerging from the specimen and hitting the objective are bundled in the optics and gathered by a light sensitive sensor behind the beam splitting mirror. Due to the small depth of field of the optics only small regions of the object are sharply imaged. To allow for a complete detection of the surface with a full depth of field, the precision optic is moved vertically along the optical axis. A sensor captures a series of 2D datasets during this scanning process. This means that each region of the object is sharply focused. All sensor parameters are optimized at each vertical position according to the reflective properties of the surface. After the scanning process, the 2D datasets are evaluated to generate 3D information. This is achieved by analyzing the variation of focus along the vertical axis. Due to the large amount of data, mechanical restrictions can be eliminated, allowing measurement results with a high resolution. Once all height measurements are determined, an image with full depth of field is computed. A key characteristic of the system is that it does not only deliver topographical information but also an optical colour image of the surface. The technology on which the system is based has recently been included into ISO standards [24] classifying different methods for surface texture extraction [25]. Five different objectives were used: ×5, ×10, ×20, ×50 and ×100 giving a lateral resolution of 1.6 μm, 800 nm, 400 nm, 160 nm and 80 nm, respectively. The image resolution is 1024 × 1280 pixels. A typical measurement lasts 1 min.

**Table 1**
Physical paper properties

| | Q− | Q+ | C | JET− | JET+ |
|---|---|---|---|---|---|
| Basis-weight (g/m$^2$) | 81.2 | 120.4 | 114.7 | 126.8 | 255.6 |
| Thickness (μm) | 110.8 | 124.7 | 92.0 | 163.6 | 273.0 |
| PPS (μm) | 5.8 | 3.2 | 1.8 | 3.4 | Out of range |
| Bendtsen (mL/min) | 129.6 | 25.0 | 13.9 | 38.9 | OOR |
| Bekk (s) | 16.9 | 109.2 | 517.1 | 93.8 | >20,000 |

### 2.3. Metallization

Some papers cannot be directly measured with the infinite focus because of a layer of transparent polymer (like latex or varnishes) on the surface. Even for non-coated paper at high magnification (×50 or ×100) the measurements can be corrupted by the translucency of the fibers. To overcome this problem, paper was metallized. Metallization consisted in fixing a thin layer (∼5 nm) of gold on the surface of the sample. This technique is often used for electronic scanning microscopy. This treatment recovers the translucent surface without corrupting the surface topography. Therefore varnished papers can be measured.

Three metallization times were chosen for each paper: 1, 2 and 4 min. These papers were then measured with the infinite focus with ×50 and ×100 magnifications. Visual inspections show that when a long time of metallization (4 min) is used, the structure of the top layer is damaged: the varnished layer cracked and some fibres burnt. However, for the 1 and 2 min time metallization, no transformation of the surface, except the colour, was found. To validate the method, 10 samples of paper Q+ were measured with and without metallization and no significant difference between the two sets of measurements were observed.

## 3. Multi-scale analysis of the surface roughness parameters

### 3.1. Comparison of roughness measurement with both air leakage methods and an optical profilometer

In the paper industry, the surface roughness of paper is often characterized using an air leakage device. These techniques are fast, easy to use and the equipment is inexpensive. The main apparatus are the Bekk, the Bendtsen and the PPS. Optical profilometry consists of a white light source, a lens, a spectrophotometer, a signal processing system, coupled with a motorized stage and an appropriate image analysis software (Papermap® expert). The sample size can be adjusted. Here, the analyzed surface was a 2 mm × 2 mm square, with a measurement spacing of 1 μm.

To validate the feasibility of the measure, the results obtained with the IFM are compared to the classical air leakage technique and to the values obtained with the Altisurf for the five papers considered in this study. Table 2 presents the correlation coefficient between the roughnesses of papers measured by the different methods.

A good correlation exists between the PPS and the optical profilometer (which has been already reported [26]).

However, the best correlation is obtained between the Altisurf and IFM results. Table 2 demonstrates the feasibility of the IFM device to characterize paper surface topography.

### 3.2. Choice of the relevant statistical parameters

For all the considered papers, 20 measurements were performed for the ×5, ×10, ×20, ×50, and ×100 magnifications. From the standard parameters we selected few surface parameters: seven amplitude parameters namely $S_q$, $S_{sk}$, $S_{ku}$, $S_p$, $S_v$, $S_z$, and $S_{10z}$, two hybrids parameters $S_{dq}$ and $S_{dr}$ and nine volume parameters $S_k$, $S_{pk}$, $S_{vk}$, $S_{mr1}$, $S_{mr2}$, $V_{mp}$, $V_{mc}$, $V_{vc}$, and $V_{rc}$. These parameters are presented in Appendix A.

**Table 2**
Correlation coefficients between the roughness of papers by different methods

| | PPS (μm) | Bendtsen (mL/min) | Bekk (s) | $S_q$ IFM ×5 | $S_q$ IFM ×10 | $S_q$ IFM ×20 | $S_q$ IFM ×50 | $S_q$ Altisurf |
|---|---|---|---|---|---|---|---|---|
| PPS | 1.000 | | | | | | | |
| Bendtsen | 0.899 | 1.000 | | | | | | |
| Bekk | −0.945 | −0.707 | 1.000 | | | | | |
| $S_q$ ×5 | 0.903 | 1.000 | −0.714 | 1.000 | | | | |
| $S_q$ ×10 | 0.973 | 0.975 | −0.846 | 0.977 | 1.000 | | | |
| $S_q$ ×20 | 0.974 | 0.975 | −0.846 | 0.977 | 1.000 | 1.000 | | |
| $S_q$ ×50 | 0.996 | 0.934 | −0.913 | 0.937 | 0.990 | 0.990 | 1.000 | |
| Altisurf | 0.997 | 0.928 | −0.919 | 0.932 | 0.988 | 0.988 | 1.000 | 1.000 |

All the parameters presented in this paper are calculated according to the mean plan. However, no filter or correction was applied: all the calculations were carried out from the raw data obtained with the IFM. Hence it is possible to compare the results obtained at different magnifications. The size of a pixel varies from 1.6 μm for the (×5) magnification down to 80 nm for the (×100) objective.

The average, the standard deviation and the relative dispersion were calculated for the papers considered. Twenty measurements by paper grade and magnification were carried out.

The main objective of these measures was to determine the relevance of the statistical parameters in the case of the paper surface topography study. Hence to be acceptable, a parameter should be reproducible and shall permit the discrimination between the different paper grades. We arbitrary fixed that a parameter was reproducible if its relative dispersion was less than 10%. The relative dispersion is defined as $(\Delta x)_{\text{rel}} = \sigma_n^2/\bar{x} \times 100$, where $\bar{x}$ represents the mean and $\sigma_n$ the standard deviation.

For all the parameters, and all the papers considered, the relative dispersion increases with the magnification. In the mean time, the overall $S_q$ value decreases with the increasing magnification (see Section 4.3). The following conclusions are consistent considering a magnification of ×5, ×10 or ×20.

For the surface parameters, only $S_q$ (and $S_a$ which is by definition related to $S_q$) fulfils the conditions. $S_{ku}$ failed for most of the papers and magnifications. $S_{dr}$ and $S_{dq}$ are stable but do not allow for distinguishing the paper quality. The skewness ($S_{sk}$) is versatile, it permits a distinction of the various qualities tested (all the paper qualities own a negative $S_{sk}$). Nevertheless, the reproducibility depends on the grade and on the magnification.

The nine volume parameters considered seem fully reproducible; the relative dispersion is essentially comprised of rates between 0 and 5. The different paper grades could be easily distinguished with the use of those parameters. Especially with $S_k$ (the core roughness) which is two times bigger for Q− than Q+. The $V_{vv}$ is also crucial as it represents the volume of the valleys. As expected the $V_{vv}$ is bigger for Q− than for Q+. Hence volume parameters are representative of a given paper quality.

Table 3 summarized the relative dispersion of the parameters according to the paper grade and to the magnification. The star on the right hand column indicates that the parameter is relevant in the characterization of the paper surface. The sign ∞ concerns parameters that are partially efficient for the discrimination, but failed under large magnifications.

## 4. Multi-scale roughness analysis

The measurement and the analysis of paper surface roughness are crucial for most of the end uses of the products. The value of the roughness is strongly dependent on the evaluation length and on the discretization (which is the length between two consecutive measured points) of the measurements. As seen in the first part, there are numerous parameters aiming to describe a surface. In the context of papermaking, one mainly focuses on the geometric average height ($R_q$ and $S_q$). However the effect of the evaluation length and the discretization is not taking into account. Small-scale measurements are often associated with optical properties of paper such as gloss while large-scale [27–29] measurements are dedicated to the characterization of surface homogeneity and machinability [22].

**Table 3**
Relative dispersions of the 19 parameters measured on three papers samples (C, Q+ and Q−)

| Relative dispersion (%) | C ×5 | C ×10 | C ×20 | Q+ ×5 | Q+ ×10 | Q+ ×20 | Q− ×5 | Q− ×10 | Q− ×20 | Relevant |
|---|---|---|---|---|---|---|---|---|---|---|
| $S_a$ (μm) | 0.5 | 0.7 | 1.4 | 0.6 | 1.6 | 6.7 | 3.7 | 8.6 | 8.6 | * |
| $S_q$ (μm) | 0.7 | 1.1 | 1.5 | 0.9 | 1.8 | 6.7 | 4.0 | 11.4 | 11.6 | * |
| $S_p$ (μm) | 44.2 | 6.2 | 13.2 | 405 | 12.2 | 351 | 129.4 | 101.0 | 244.2 | |
| $S_v$ (μm) | 47.0 | 45.5 | 277.0 | 1141 | 51.6 | 58.4 | 48.9 | 63.5 | 75.3 | |
| $S_z$ (μm) | 58.0 | 35.7 | 210.1 | 717.5 | 40.3 | 203 | 98.7 | 77.7 | 152.2 | |
| $S_{10z}$ (μm) | 27.9 | 28.3 | 214.2 | 76 | 30.7 | 54.7 | 33.0 | 66.2 | 73.7 | |
| $S_{sk}$ | −8.5 | −33.4 | −72.0 | −6.6 | −4.5 | −47.7 | −10.0 | −2.8 | −5.4 | ∞ |
| $S_{ku}$ | 6.5 | 716.0 | 996.3 | 61 | 51.7 | 805 | 4.5 | 11.7 | 12.9 | |
| $S_{dq}$ | 0.0 | 0.2 | 4.6 | 0.0 | 0.1 | 3.4 | 0.0 | 0.5 | 6.3 | * |
| $S_{dr}$ (%) | 1.6 | 3.3 | 64.2 | 0.9 | 8.2 | 138 | 3.5 | 32.2 | 513.7 | ∞ |
| $S_k$ (μm) | 1.8 | 1.7 | 7.5 | 1.7 | 7.3 | 23.7 | 16.6 | 19.8 | 28.6 | ∞ |
| $S_{pk}$ (μm) | 1.5 | 3.3 | 5.5 | 1.4 | 3.6 | 9.2 | 5.0 | 9.5 | 10.7 | * |
| $S_{vk}$ (μm) | 1.6 | 5.3 | 6.2 | 3.1 | 2.3 | 11.4 | 2.7 | 34.2 | 27.2 | * |
| $S_{mr1}$ | 1.5 | 12.7 | 2.2 | 1.6 | 9.2 | 28.5 | 6.8 | 13.5 | 51.7 | * |
| $S_{mr2}$ | 0.4 | 1.5 | 5.3 | 0.2 | 1.6 | 4.6 | 1.7 | 3.6 | 4.4 | * |
| $V_{mp}$ | 0.1 | 0.2 | 0.3 | 0.1 | 0.1 | 0.2 | 0.3 | 0.3 | 0.3 | * |
| $V_{mc}$ | 0.5 | 0.8 | 1.5 | 0.6 | 2.0 | 9.2 | 5.5 | 10.0 | 9.8 | * |
| $V_{vc}$ | 0.9 | 0.6 | 2.8 | 0.7 | 2.4 | 8.2 | 6.6 | 8.9 | 13.6 | * |
| $V_{vv}$ | 0.2 | 0.5 | 0.6 | 0.3 | 0.3 | 1.1 | 0.3 | 3.6 | 3.0 | * |

### 4.1. Algorithms of the multi-scale roughness analyses

From the surface measurements of the five papers selected for the study, the geometric average height ($S_q$) was calculated independently as a function of both the evaluation length (defined as the length of the edge of the square where the calculation is performed) and the step of discretization.

The measurements consisted in $1024 \times 1024$ pixels (noted $L \times L$) with a step of discretization of 1600 nm, 800 nm, 400 nm, 160 nm and 80 nm for the magnification $\times 5$, $\times 10$, $\times 20$, $\times 50$ and $\times 100$, respectively.

The algorithm, developed for the multi-scale study computed the value of $S_q$, $S_{sk}$, $Y_{\min}$ and $Y_{\max}$ for a given evaluation length $l$ and a given position $(x,y)$ for the surface referred to as $i$. $Y_{\min}$ and $Y_{\max}$ are the minimum and maximum values of the considered surface. A step of growth for the evaluation length is chosen, $\Delta = \Delta x = \Delta y = 1$ pixel. The first step is to divide the initial surface into equally sized squares with edges of $l_0$ ($l_0$ is taken equal to 2 $\mu$m). Then for each of these squares (indexed as $t$) local values of $S_q^t(l_0, i)$, $S_{\rm sk}^t(l_0, i)$, $S_{\rm ku}^t(l_0, i)$, and $R^t = Y_{\max}(l_0,\ i) - Y_{\min}(l_0,\ i)$ are calculated according to the local mean plan. Then the local values are averaged to calculate $S_q(l_0,\ i)$, $S_{sk}(l_0,\ i)$, $S_{ku}(l_0,\ i)$ and $R(l_0)$ corresponding to the observation scale $l_0$. Then new squares are extracted from the original surface $i$ with an edge of $l_1 = l_0 + \Delta$. The operation is repeated until $l_n = L$.

From the profile measurements only the influence of the evaluation length was considered. The measurements consisted of a length $L$ = 50,000 $\mu$m with a step of discretization of 1 $\mu$m. The same algorithm was applied to the profiles as the one used for the surfaces.

### 4.2. Fractal concepts

The dependence on the roughness regarding the evaluation length can be integrated in the fractal concept, which aims to find invariant scale parameters. The most common method for roughness analysis is based on the Mandelbrot works [30]. Fractal surfaces own a linear relation between roughness parameters and the length of evaluation in log–log representation. The slope of the curve $H = \Delta \log_{10} S_q / \Delta \log_{10} l$ is related to the Holder exponent which allows for the calculation of the fractal dimension $F$ of the considered surface ($F = 2 - H$). The fractal behaviour of paper surfaces was studied using several approaches [17,3,20]. Nevertheless no clear conclusions were drawn on this subject. In the next part, we will investigate the fractal behaviour of the paper surface roughness. As the paper roughness is size dependent, the fractal concept could be a tool to obtain invariant roughness descriptors. To visually emphasise the possible fractal behaviour of paper surface, Fig. 1 presents a profile recorded with the profilometer of the paper Q− with three spatial zooms ($\times 5$, $\times 25$ and $\times 125$) located at the origin of the profile plot.

### 4.3. Profile analysis

The figure presents the multi-scale roughness values of $S_q$, $R$, and $S_{sk}$ for paper C (to facilitate the reading only five samples are plotted which were extracted from the 20 profiles measured).

The following comments are valid for the different paper grades tested. As a matter of fact, the three parameters chosen sharply depend on the analysis length. For example the $S_q$ value is multiplied by 2 when the evaluation length varies from 2000 $\mu$m to 10,000 $\mu$m. The values of $S_q$ and Amp seem to increase logarithmically. No clear stabilization is reached even for large evaluation lengths (above 10,000 $\mu$m). The final range of values of the skewness for the same paper is large and comprised between

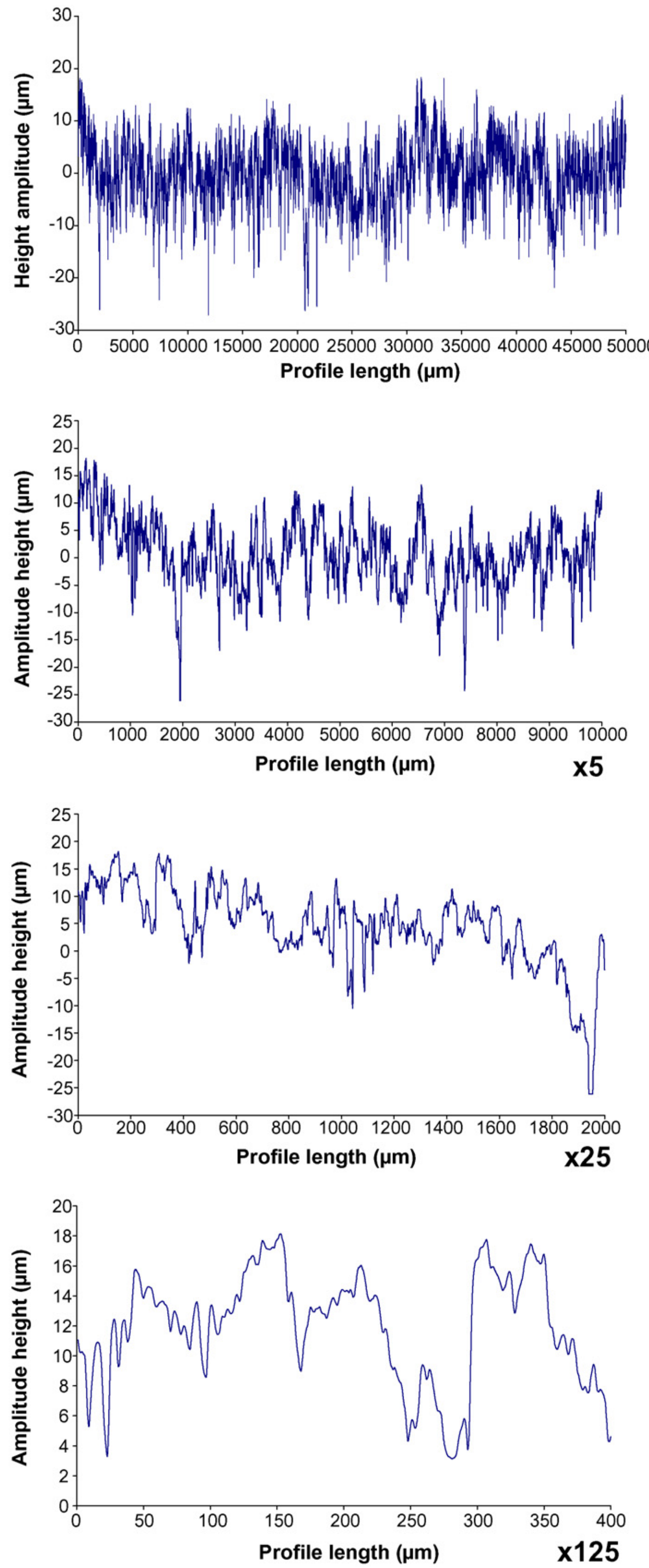


**Fig. 1.** Recorded profile of paper Q− with three spatial zooms (×5, ×25, and ×125) located at the origin of the whole profile.

−1.65 and 0.1. As a matter of fact (Fig. 2c) the shape of the $S_{sk}$ evolution is irregular and some variations appear on the graph. The usefulness and the relevancy of such a parameter for the description of paper surface are therefore questioned.

For the three parameters considered in Fig. 1, the curves are more and more scattered while the evaluation length increases (especially when $l > 1000\ \mu m$).

To evaluate fractal dimension of the parameter $S_q$ for the different papers considered in this study, an averaged $S_q$ value was calculated for the 20 profiles measured for each grade. Fig. 3 presents the variation of $S_q$ for the four papers in a log–log coordinate system.

The four considered curves present different stages in their variations. Basically the evolution can be divided into three linear stages in the log–log representation. Using the Mandelbrot theorem, the Holder exponent is calculated (for the linear stage in the log–log representation) and then the fractal dimension of each different stage is extracted. Table 4 exhibits the value of the slopes of the three stages, their domain of validity, the regression coefficient associated to each line and the fractal dimensions for the paper C, Q+, Q− and JET−.

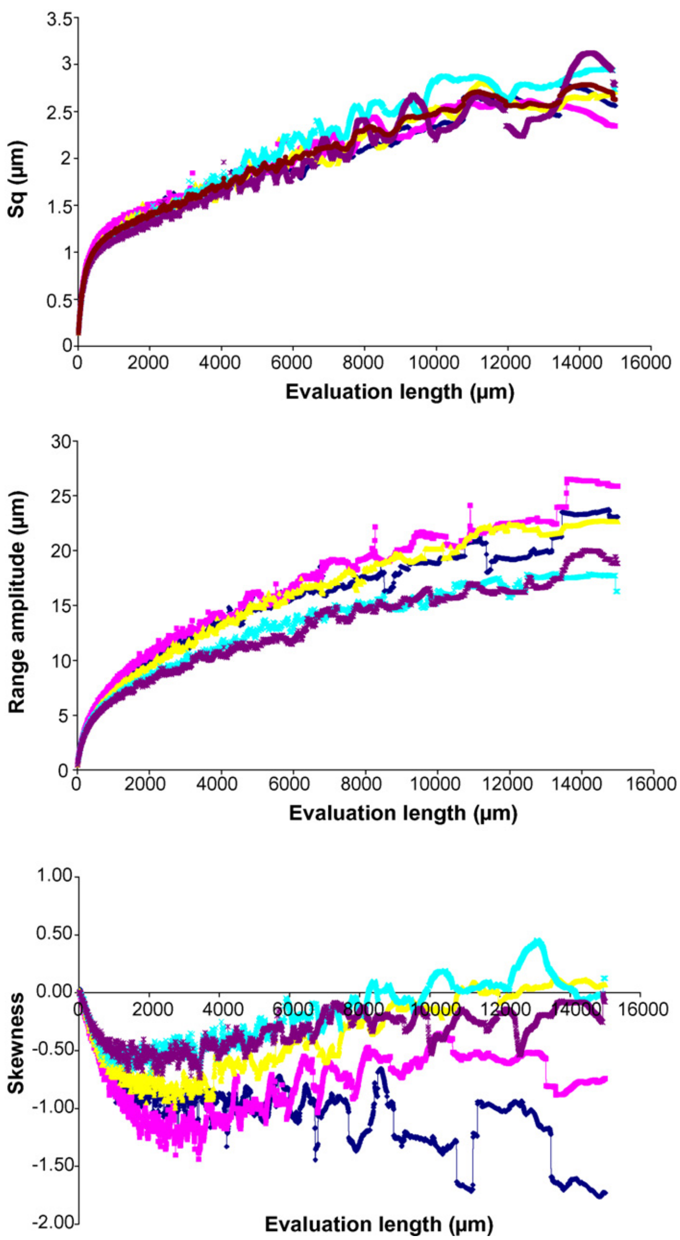


**Fig. 2.** $S_q$, $R$ and $S_{sk}$ multi-scale roughness values at different observation scales for five profiles of paper C.

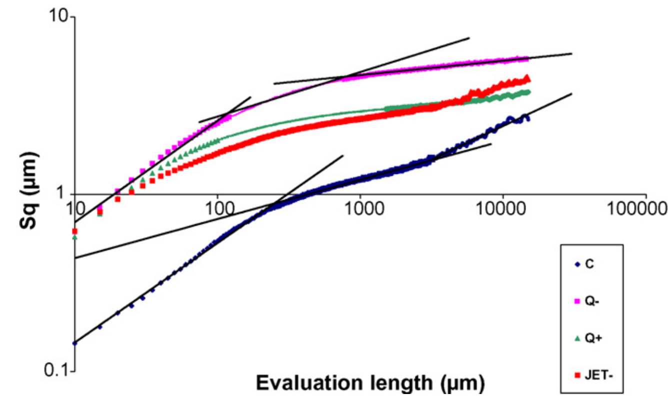


**Fig. 3.** $S_q(l)$ multi-scale analysis based on the analysis of profiles of paper C, Q−, Q+ and JET− (the linear regression from which the slopes were calculated are plotted for the paper C and Q− to illustrate the proposed method).

Some general comments on the different stages can be made from this table.

- The first stage is short (between 100 μm and 250 μm for paper Q+ and C, respectively) with a high slope value. The degree of confidence of this stage is high as the regression coefficient is 0.99 for all the paper grades.
- The length of the second stage strongly depends on the paper quality. As a matter of fact the quality of the linear regression is high (except for the paper Q+ for which $R^2 = 0.97$). The domain range of this stage varies from 750 μm to 3500 μm.
- The third stage deals with long length analysis roughness. The value of the regression coefficient is not as high as for the two previous stages. For the two uncoated papers (Q+ and Q−) the slopes of this last stage are small (around 0.1), contrary to the two coated papers (JET− and C) which have a large value of slopes. We assume that the coating process and especially the drying process create large-scale undulation of the papers which is responsible for these large slopes.

Several studies on roughness dependency related to the evaluation length reported comparable behaviours [23,31,32].

**Table 4**
Determination of the roughness stages and their associated fractal coefficients

| Paper | Stage 1 | Stage 2 | Stage 3 |
|---|---|---|---|
| C | | | |
| Slope | **0.56** | **0.22** | **0.37** |
| $R^2$ | 0.99 | 0.99 | 0.98 |
| Range of validity (μm) | 1–250 | 250–3200 | 3200–15000 |
| Q− | | | |
| Slope | **0.57** | **0.25** | **0.08** |
| $R^2$ | 0.99 | 0.99 | 0.98 |
| Range of validity (μm) | 1–120 | 120–750 | 750–15000 |
| Q+ | | | |
| Slope | **0.52** | **0.13** | **0.10** |
| $R^2$ | 0.99 | 0.97 | 0.97 |
| Range of validity (μm) | 1–100 | 100–1500 | 1500–15000 |
| JET− | | | |
| Slope | **0.38** | **0.13** | **0.25** |
| $R^2$ | 0.99 | 0.99 | 0.98 |
| Range of validity (μm) | 1–150 | 150–3500 | 3500–15000 |

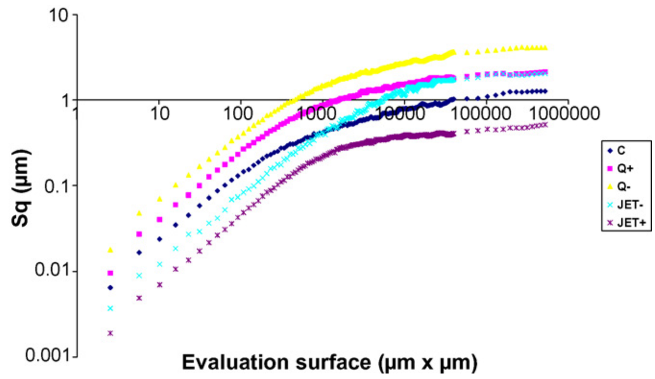


**Fig. 4.** $S_q(l)$ multi-scale analysis based on the analysis of surface mapping of paper C, Q−, Q+ and JET− at a magnification of ×10.

For examples, Bigerelle et al. [21] studied the roughness of precision machined surfaces, Ganti and Bhusnan [33] analysed magnetic tape and disk, while Pollion and Grenet [34] focused on steel surfaces. The knowledge of the various stages of the curves presented in Fig. 3 allows for the prediction of the length dependency of a surface. In some studies [31], the last stage was not linear anymore and was fitted by a logarithmic function in log–log representation. Hence it permits the development of a model fitting this logarithmic stage using a generalized lambda distribution (GLD) as presented in [21].

### 4.4. Surface analysis

The analysis of profile roughness demonstrated the importance of the analysis length in the variation in the values of the roughness parameters. We will now discuss the nature of the dependency for square (which is the common surface geometry chosen to describe paper roughness). The step of discretization represents another crucial factor. Thanks to the algorithm described in Section 4.1, paper roughness variation was studied in relation to both the evaluation length (which in this case is the length of the edge of a square) and the step of discretization.

Fig. 4 shows the variations of $S_q$ for the five papers and a magnification of ×10 in a log–log representation.

The influence of the surface size in the variation of $S_q$ is demonstrated in this graph. The three stages described in Section 4.3 are visible. Hence the knowledge (or the calculation) of the various slopes of the curves shall allow for a prediction of the roughness as a function of the evaluation surface size. The paper JET− presents an interesting variation: for small evaluation surface size (<1000 $\mu m^2$) it is smoother than C but then an inversion occurs and its final roughness for larger size (>100,000 $\mu m^2$) is superior to paper C.

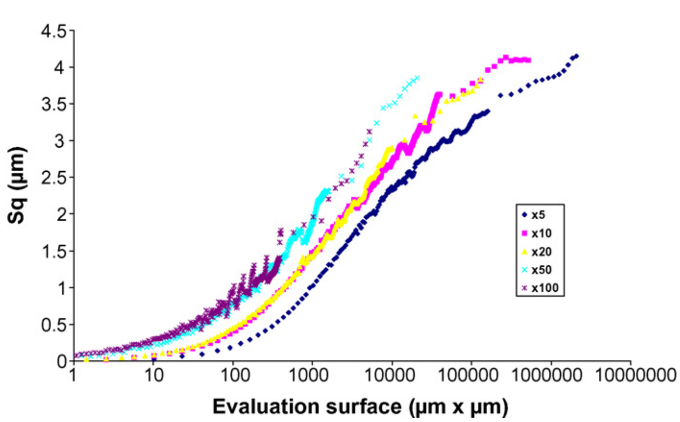


**Fig. 5.** $S_q(l)$ multi-scale analysis based on the analysis of surface mapping of paper Q− for magnification ×5, ×10, ×20, ×50 and ×100, respectively.

Fig. 5 presents the $S_q$ variations for the paper Q− as a function of both the surface size and the step of discretization in a semi-log representation. The other paper studied present similar shape and behaviour.

The influence of the step of discretization is shown in this graph. As a matter of fact, for a given surface size, the $S_q$ value of the paper is strongly dependent on this discretization: hence the multi-scale behaviour is confirmed. Unsurprisingly, the highest roughness values are obtained for the biggest discretization steps. Therefore, this representation allows for the quantification of the relationship between the roughness value and the surface size of the sample.

## 5. Conclusions

A focus variation device allows for measurements to be taken of the paper surface topography at various scales. A study of the relevancy of statistical roughness parameters was performed.

From the initial 19 parameters tested, 11 present both a good reproducibility and allow for the distinguishing of the different paper grades studied for all the magnification tested.

A multi-scale analysis based on scaling analysis was performed. The influence of both the length of analysis and the step of discretization was studied. The method introduced in this paper, based on fractal analysis, was applied on both paper profiles and paper surfaces. We therefore demonstrated that the root mean square ($S_q$) variation of paper surfaces follows three different stages according to the length of evaluation of the sample. From an industrial point of view, a better knowledge of the paper surface roughness could reduce the time of measurements processing, and may also lead to future inline measurements. Along with this, the quality of the measurements may also be improved. Future works should relate the scale of roughness to be considered to particular properties of paper, such as friction, gloss or ink transfer.

## Appendix A. Definition of surface parameters

$S_q$ is a dispersion parameter defined as the root mean square value of the surface departures within the sampling area.

$$S_q = \sqrt{\frac{1}{MN}\sum_{j=1}^{N}\sum_{i=1}^{M}|z|^2(x_i, x_j)} \quad (1)$$

where $M$ is a number of points of per profile and $N$ is the number of profiles. $S_q$ is a general and widely used parameter.

$S_{sk}$ is the measure of asymmetry of surface deviations about the mean plane.

$$S_{sk} = \frac{1}{MNS_q^3}\sum_{j=1}^{N}\sum_{i=1}^{M}|z|^3(x_i, x_j) \quad (2)$$

This parameter can effectively be used to describe the shape of the topography height distribution. For a Gaussian surface which has a symmetrical shape for the surface height distribution, the skewness is zero. For an asymmetric distribution of surface heights, the skewness may be negative if the distribution has a longer tail at the lower side of the mean plane or positive if the distribution has a longer tail at the upper side of the mean plane. The knowledge of the asymmetric behaviour of a paper surface is relevant for example for the control of the friction.

$S_{ku}$ is a measure of the peakedness or sharpness of the surface height distribution.

$$S_{ku} = \frac{1}{MNS_q^4} \sum_{j=1}^{N} \sum_{i=1}^{M} |z|^4 (x_i, x_j) \tag{3}$$

This parameter characterizes the spread of the height distribution. A Gaussian surface has a kurtosis value of 3. A centrally distributed surface has a kurtosis value larger than 3 whereas the kurtosis of a well spread distribution is smaller than 3. By a combination of the skewness and the kurtosis, it may be possible to identify surfaces which have a relatively flat top and deep valleys. Material volume and void volume in the surface bearing area is a naturally geometrical descriptor of a surface topography [16]. The material volume and void volume enclosed in the contacting surface of the material, they may have a close relation with functional properties of the surface, such as bearing, wear and fluid retention. The volume parameters are derived from the bearing area analysis of the complete 3D surface. The bearing area curve is formed by establishing the amount of material a plane would rest on relative to the complete cross section of the surface for each height from the highest to the lowest point of the surface [35]. Volume parameters are deduced from the bearing curve [36] according to the Blunt's recommendations [37].

## References

[1] J.F. Bloch, S. Rolland du Roscoat, C. Mercier, P. Vernhes, B. Pineaux, A. Blayo, P. Mangin, Influence of paper structure on printability: characterisation using X-ray synchrotron microtomography, presented at NIP, Denver, USA, 2006.
[2] P. Vernhes, C.-S. Rolland du Roscoat, A. Blayo, B. Pineaux, J.F. Bloch, Synchrotron X-ray microtomography: a new tool to characterize the interaction between paper and toner, J. Imaging Sci. Technol. 52 (2008) 6.
[3] G. Chinga, Detailed characterization of paper surface structure for gloss assessment, J. Pulp Paper Sci. 30 (2004) 222–227.
[4] G. Chinga, T. Helle, Relationships between the coating surface structural variation and print quality, J. Pulp Paper Sci. 29 (2003) 179–184.
[5] J.S. Arney, H. Heo, R.G. Anderson, A micro-goniophotometer and the measurement of print gloss, J. Imaging Sci. Technol. 48 (2004) 458–463.
[6] J.S. Arney, J. Michel, K. Pollmeier, Technique for analysis of surface topography of photographic prints by spatial analysis of first surface reflectance, J. Imaging Sci. Technol. 46 (2002) 350–358.
[7] J.S. Arney, L. Ye, J. Wible, T. Oswald, Analysis of paper gloss, J. Pulp Paper Sci. 32 (2006) 19–23.
[8] M.C. Beland, S. Lindberg, P.A. Johansson, Optical measurement and perception of gloss quality of printed matte-coated paper, J. Pulp Paper Sci. 26 (2000) 120–123.
[9] M.C. Beland, L. Mattsson, Optical print quality of coated papers, J. Pulp Paper Sci. 23 (1997) J493–J498.
[10] T. Pettersson, A. Fogden, Leveling during toner fusing: effects on surface roughness and gloss of printed paper, J. Imaging Sci. Technol. 50 (2006) 202–215.
[11] I. Arino, U. Kleist, G.G. Barros, P.A. Johansson, M. Rigdahl, Surface texture characterization of injection-molded pigmented plastics, Polym. Eng. Sci. 44 (2004) 1615–1626.
[12] P. Aslund, P.A. Johansson, E. Blohm, Photometric method for dynamic measurements of paper roughening after a moistening printing nip, Nord. Pulp Paper Res. J. 19 (2004) 460–465.
[13] J.S. Aspler, M.C. Beland, A review of fiber rising and surface roughening effects in paper, J. Pulp Paper Sci. 20 (1994) J27–J32.
[14] G. Chinga, T. Stoen, O.W. Gregersen, On the roughening effect of laboratory heatset offset printing on SC and LWC paper surfaces, J. Pulp Paper Sci. 30 (2004) 307–311.
[15] S. Hartmuth, S. Mario, S. Stefan, Comparison of 3D surface reconstruction data from certified depth standards obtained by SEM and an infinite focus measurement machine (IFM), Microchim. Acta V155 (2006) 279–284.
[16] F. Raharijaona, X. Roizard, J. von Stebut, Usage of 3D roughness parameters adapted to the experimental simulation of sheet–tool contact during a drawing operation, Tribol. Int. 32 (1999) 59–67.
[17] G. Chinga, A quadtree decomposition approach for surface assessment, Pattern Anal. Appl. V 9 (2006) 94–101.
[18] H. Granberg, M.C. Beland, Modelling the angle-dependent light scattering from sheets of pulp fibre fragments, Nord. Pulp Paper Res. J. 19 (2004) 354–359.
[19] C. Antoine, G. Chinga, Wavelet analysis of paper surface structure, presented at Progress in Paper Physics Seminar, Trondheim, 2004.
[20] H. Kent, The fractal dimension of paper surface topography, Nord. Pulp Paper Res. J. (1991) 191–196.
[21] M. Bigerelle, A. Gautier, A. Iost, Roughness characteristic length scales of micromachined surfaces: a multi-scale modelling, Sens. Actuators B 126 (2007) 126–137.
[22] R.M. Patrikar, Modeling and simulation of surface roughness, Appl. Surf. Sci. 228 (2004) 213–220.
[23] J.-J. Wu, Characterization of fractal surfaces, Wear 239 (2000) 36–47.
[24] ISO 25178-6, Geometrical product specifications (GPS)–surface texture: Areal–Part 6: Classification of methods for measuring surface texture.
[25] F.H.R. Danzl, Three-dimensional reconstruction of surfaces with steep slopes using an optical measurement system based on a colour focus sensor, presented at 6th International Euspen Conference, 2006.
[26] R. Xu, P. Fleming, A. Pekarovicova, The effect of ink jet paper roughness on print gloss, J. Imaging Sci. Technol. 49 (2005) 660–666.
[27] T.R. Lettieri, E. Marx, J. Song, T.V. Vorburger, Light scattering from glossy coatings on paper, Appl. Opt. 30 (1993) 4439–4447.
[28] M.C. Beland, J. Bennet, Effect of local microroughness on the gloss uniformity of printed paper surfaces, Appl. Opt. 39 (2000) 2719–2726.
[29] V. Bliznyuk, H. Assender, K. Porfyrakis, How surface topography relates to material's properties, Mater. Sci.: Soft Surf. 297 (2002) 973–976.
[30] B. Mandelbrot, Self-affine fractals and fractal dimension, Phys. Scripta 32 (1985) 257–260.
[31] J.-J. Wu, Simulation of rough surfaces with FFT, Tribol. Int. 33 (2000) 47–58.
[32] N. Patir, A numerical procedure for random generation of rough surfaces, Wear 47 (1978) 263–277.
[33] S. Ganti, B. Bhusnan, Generalized fractal analysis and its applications to engineering surfaces, Wear 180 (1995) 17–34.
[34] P. Pollion, G. Grenet, Determination of fractured steel surface roughness by atomic force microscopy using fractal based approach, Surf. Interf. Anal. 24 (1996) 282–285.
[35] F. Sacerdotti, B. Griffiths, F. Benati, H. Kang, The variability of functional and amplitude three-dimensional roughness parameters for electron-beam and electro-discharged textured surfaces, Meas. Sci. Technol. 11 (2000) 171–177.
[36] M. Bigerelle, A. Iost, A numerical method to calculate the Abbott parameters: a wear application, Tribol. Int. 40 (2007) 1319–1334.
[37] J. Blunt, Assessment of surface topography, 2003.